Conversion of light into macroscopic helical motion

Supitchaya Iamsaard[1], Sarah J. Aßhoff[1], Benjamin Matt[1], Tibor Kudernac[2], Jeroen J. L. M. Cornelissen[1], Stephen P. Fletcher[3]* and Nathalie Katsonis[1]*

A key goal of nanotechnology is the development of artificial machines capable of converting molecular movement into macroscopic work. Although conversion of light into shape changes has been reported and compared to artificial muscles, real applications require work against an external load. Here, we describe the design, synthesis and operation of spring-like materials capable of converting light energy into mechanical work at the macroscopic scale. These versatile materials consist of molecular switches embedded in liquid-crystalline polymer springs. In these springs, molecular movement is converted and amplified into controlled and reversible twisting motions. The springs display complex motion, which includes winding, unwinding and helix inversion, as dictated by their initial shape. Importantly, they can produce work by moving a macroscopic object and mimicking mechanical movements, such as those used by plant tendrils to help the plant access sunlight. These functional materials have potential applications in micromechanical systems, soft robotics and artificial muscles.

The promise of developing artificial molecular machines has inspired scientists for decades[1,2] and led to the design and operation of small molecules that exhibit mechanically relevant movements, such as rotation[3–6], walking[7] and twisting[8], as well as more-complex molecular-scale operations, such as driving[9] and chemical synthesis[10]. Rudimentary examples of nanomachines capable of work[11–15] provide tantalizing hints of the potential power of molecular devices. However, materials capable of translating molecular motion into useful macroscopic function remain elusive[16–19].

Nature uses molecular-scale machines to drive every significant biological process[20] and powers macroscopic mechanical motion in plants in highly complex processes[21]. Examples of biological systems built on helical motion include powerful engines such as spasmoneme springs[21], seed pod opening[22] and tendril coiling[23].

Based on the general concept that such plant-like helical deformations may similarly occur in artificial systems, which thus makes them capable of producing mechanical work, we set out to design a system in which molecular movement would be translated across scale lengths into macroscopic rotational movement, and form the basis of functional materials. Previous studies reported on a light-induced film twisting of thin crystals[24,25] and out-of-plane deformations of polymer films controlled by irradiation with polarized light[26]. In these examples, selective irradiation was necessary to control the twisting mechanism. In contrast, here we seek to create smart materials with photoresponses inherently encoded in their structure.

Results and discussion

Amplifying molecular chirality in a liquid-crystal polymer network. Our approach involves using a liquid-crystal polymer network[27] that can selectively form either right-handed or left-handed macroscopic helices at room temperature. Liquid-crystal polymer networks display a strong coupling between orientational order and mechanical strain, which is why they undergo deformations when submitted to a stimulus-induced decrease of order. Light is an especially attractive stimulus to induce such macroscopic modifications, as it has proved to be a versatile and

controllable energy source for driving a wide range of nanoscale molecular systems[11,12,15–18]. Arguably, the most straightforward manner to induce light responsiveness in a polymer network is to introduce light-responsive switches, such as azobenzene units[28–30], into its covalent structure. Molecular switch **1** (Fig. 1a) is an azobenzene-based photochromic switch that undergoes *trans–cis* photoisomerization under irradiation with ultraviolet light (Supplementary Fig. 1). The switch acts as a nanoscale energy converter and is incorporated into the polymer network through polymerizable acrylate groups. It has been shown that for azobenzene concentrations up to 10 wt%, photoinduced deformations scale with the concentration of the azobenzene[31], and thus the concentration of **1** in the polymer network was set to 10 wt% to provide large photoinduced deformations.

The host matrix we used is based on a combination of a low molecular-weight nematic liquid crystal (commercially available E7) and acrylate-functionalized nematic liquid crystals that photopolymerize in the presence of an initiator (Supplementary Fig. 2). We selected a photoinitiator that absorbs at wavelengths longer than 420 nm to achieve cross-polymerization while minimizing the isomerization of **1**. A small amount of the chiral dopant (**S-811**, Fig. 1b) was added to the liquid-crystalline mixture to favour a left-handed twist (Fig. 1c). The mixture was then introduced into a glass cell to promote a twist geometry, in which the orientation of the liquid-crystal director changes smoothly by 90° from the bottom surface to the top surface (Fig. 1c,d). Polarized optical microscopy shows that the molecular organization of the liquid crystal is largely preserved after polymerization. After the cells were opened and the films dried, strips with a width of 0.7–0.9 mm were cut in a direction characterized by the angular offset φ defined here as the angle between the orientation of the molecules at mid-plane on one hand, and the cutting direction on the other hand, which also corresponds to the long axis of the ribbons (Figs 1c and 2). An illustration of how the films are cast and how they coil spontaneously into springs once they are cut into ribbons is provided in Supplementary Fig. 3. Below we show that the direction in which the ribbons are cut is a parameter that
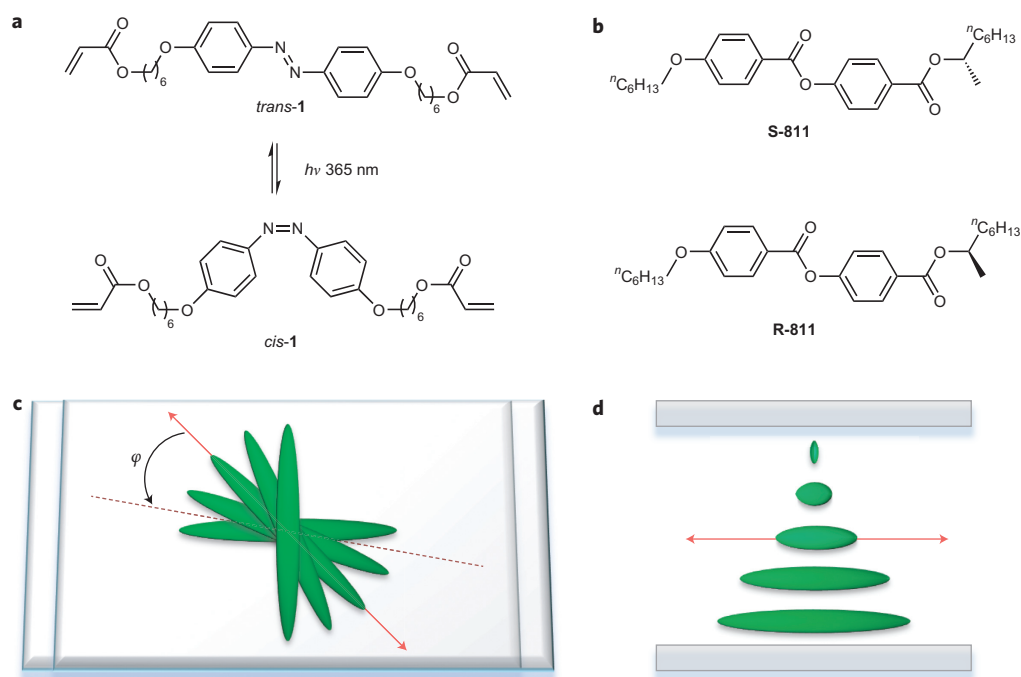
Figure 1 | A photoresponsive liquid crystal in a twist-nematic molecular organization. a, The molecular photoswitch **1** used in this study is an azobenzene derivative. **b**, Chiral dopants **S-811** and **R-811** induce a left-handed and right-handed twist in the liquid crystal, respectively. **c**, Molecular organization in the twist cell (top view) and the angular offset φ, which characterizes the angle at which the ribbon is cut. The orientation of the molecules at mid-plane is shown with a double-headed arrow. The cutting direction, which is also the long axis of the ribbon, is represented by a dotted line. The elongated rods represent molecules. **d**, The twist-nematic molecular orientation through the thickness of the film (side view).
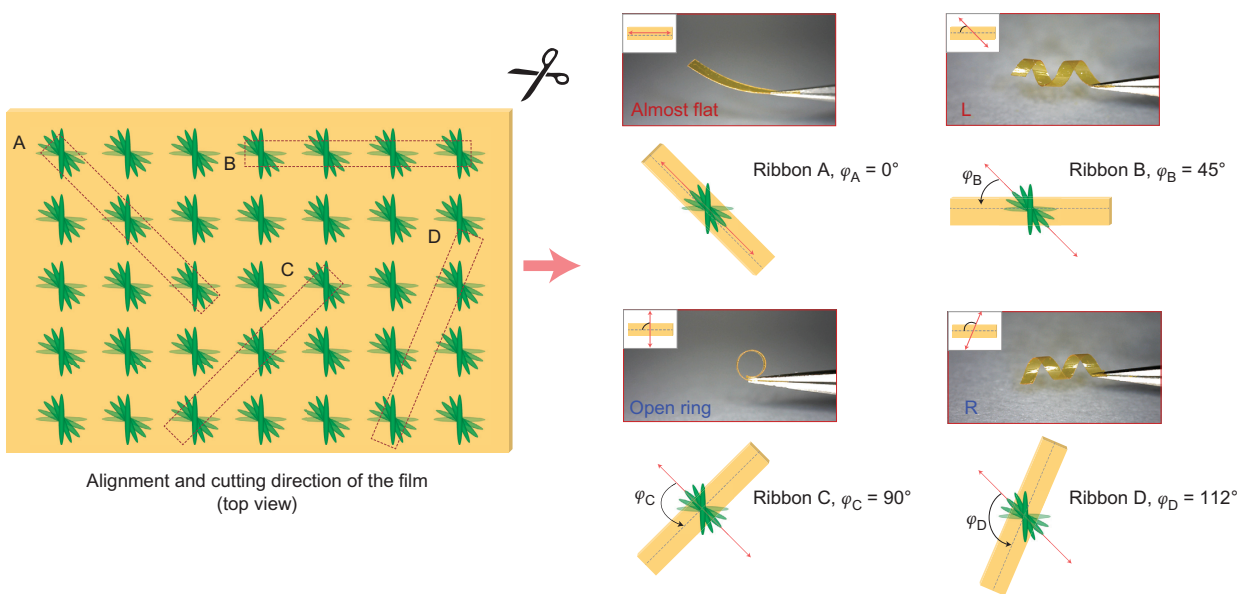

Figure 2 | The ribbons display a variety of shapes that depend on the direction in which they are cut. The samples display a rich variety of chiral shapes, from left-handed or right-handed ribbons (ribbons B and D) to ribbons for which chirality is not expressed macroscopically (flat ribbon A or open-ring ribbon C).

determines not only the pitch and handedness of the helical shapes that are formed, but also their photoresponsive behaviour.

Generating a diversity of helical shapes. On polymerization and/or drying of such a film, anisotropic shrinking occurs and leads to out-of-plane twisting once the film is released from the cell and cut into ribbons[32–34]. In particular, Urayama and co-workers presented a strain model according to which ribbons cut out from twisted nematics select a helicoid or spiral shape, depending on their

width[32]. That is, polymerization and/or drying of the ribbons induces shrinking of each face of the ribbon orthogonally to each other, and the ribbons have to curl to accommodate for it. The shrinking is anisotropic, so the shape of each ribbon is determined by the orientation of the molecules with respect to the short and long axes of the ribbons.

In the work reported here, the width of the ribbons was constant. We propose that the diversity of helical shapes we observed arises from three sources, which can reinforce or compete depending on
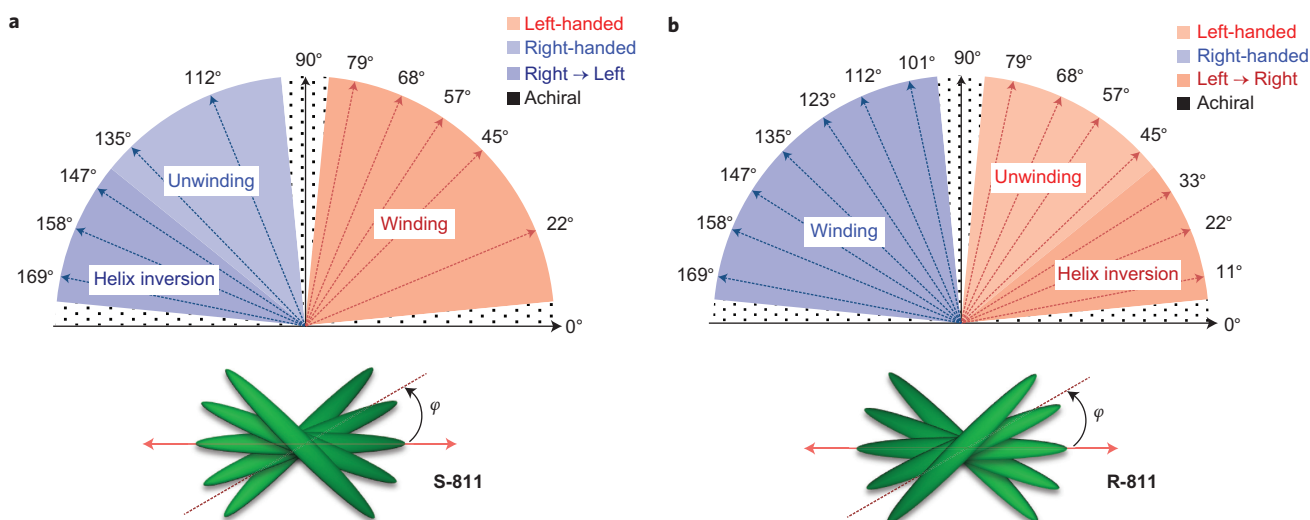
Figure 3 | Shape and photoactuation modes of the polymer springs as a function of the angular offset. The angular offset φ is defined here as the angle between the orientation of the molecules at mid-plane and the cutting direction. The experimental error is estimated to $\pm 2°$. **a**, Ribbons doped with **S-811**, in which the director twist is left-handed. **b**, Ribbons doped with **R-811**, where the director twist is right-handed. The two diagrams are symmetric with respect to the photoresponse.

the angle at which the ribbon is cut: (1) the handedness of the director twist, which is determined by the handedness of the chiral dopant, (2) the angular offset φ, which is determined by the angle at which the ribbon is cut, and (3) a gradient in density is expected through the thickness of the sample, because the films are always irradiated from the same side, that is from the top of the sample, during photopolymerization. Based on the competition between these sources of asymmetry, the samples can form a rich variety of chiral shapes, from left-handed or right-handed ribbons with diverse pitches (Fig. 2, ribbons B and D), to ribbons for which chirality is not expressed macroscopically (Fig. 2, flat ribbon A or open-ring ribbon C). Additional images for the shape selection of the ribbons are shown in Supplementary Fig. 4.

As expected, in ribbons where the chiral dopant **S-811** was replaced by its enantiomer **R-811** we observed that the shape of the ribbons was the mirror image—that is, the polymers produced were enantiomers of each other (Fig. 3 and Supplementary Fig. 5). For example, an **S-811** ribbon cut at $\varphi = 22°$ is expected to be the enantiomer of an **R-811** ribbon cut at $\varphi = 158°$ (Fig. 3), as both the handedness of the director twist and the angular offset are symmetric in these two ribbons. Indeed, we observed that the former ribbon yielded a left-handed spring, whereas the latter yielded a right-handed spring of similar pitch (Supplementary Figs 4 and 5).

In passive (non-photoactive) ribbons that have been emptied from chiral molecules and non-reacted materials, twist-free ribbons (either open-ring ribbons or flat ribbons) have been observed at $\varphi \approx 45°$ and $135°$, which is expected for a non-chiral system of orthogonally shrinking sheets[35]. In contrast, we observed achiral ribbons for $\varphi \approx 0°$ and $90°$, where the surface directors are not parallel to the axes of the ribbon but, instead, the mid-plane director is parallel to one of the axes. This difference indicates a strong source of asymmetry in the system. To verify this conclusion, we heated the ribbons to $180\,°C$ (Supplementary Figs 6 and 7). As the temperature was gradually increased, unreacted materials (E7 and chiral dopant) were expelled from the polymer network. When all these materials had diffused away, the ribbons were emptied from the additional source of asymmetry provided by **S-811** and underwent a shape transition. At $180\,°C$, the shapes we observed corresponded well to the shapes of the passive ribbons observed by Sawa *et al.*[32,33]; in particular, the shape of the $\varphi = 45°$

ribbon became achiral. Importantly, the temperature-induced shape transition that we observed was not reversible.

Surprisingly, after cutting, all the ribbons presented here curled in such a way that the area facing the top of the cell was always found on the outside of the ribbon, whereas the bottom of the film always ended up inside the twisted ribbon. This conclusion was drawn after labelling one side of the ribbons with sticky tape (Supplementary Figs 8 and 9). We propose that the preferential curling direction originates in a light-intensity gradient caused by the thickness of the sample during photopolymerization, because both the photoactive dopant and the photoinitiator are optical absorbers at $\lambda \geq 420$ nm (Supplementary Fig. 1). As the polymerization rate scales with light intensity, the reactive monomers are depleted preferentially at the top of the sample. This gradient of concentration in reactive monomers drives the diffusion of the monomers to the top of the film during polymerization and the final sample displays a higher density and cross-link density at the top[36]. To confirm that the curvature of the ribbons is influenced by a density gradient in the film, we performed photopolymerization by placing the lamp at the bottom of the sample (rather than at its top). For a fixed offset angle, we observed that the ribbons had a similar pitch, but an opposite handedness. We found that when photopolymerization occurred from the bottom, the bottom of the film always ended up outside the spiral ribbons. This observation provides insight into both the shape and the photoresponsive properties of the springs. In all the experiments described below, the ribbons were prepared by photopolymerization from the top of the cell.

To summarize, two parameters characterize the shape of the ribbons—the pitch and the bending direction. The pitch of the spiral ribbons (that is, the absolute value of the curvature) is determined by the director orientation within the ribbons. The bending direction (that is, the handedness of the spiral ribbons) is determined not only by the director orientation within the ribbons, but also by the direction of the polymer gradient.

Photoactuation modes of the helical ribbons. We investigated the photoresponse of these twisted ribbons (Figs 3 and 4). Under irradiation with light, left-handed spiral ribbons doped with **S-811** decreased in their macroscopic pitch, and the corresponding right-handed ribbons showed an increase in macroscopic pitch (Fig. 4
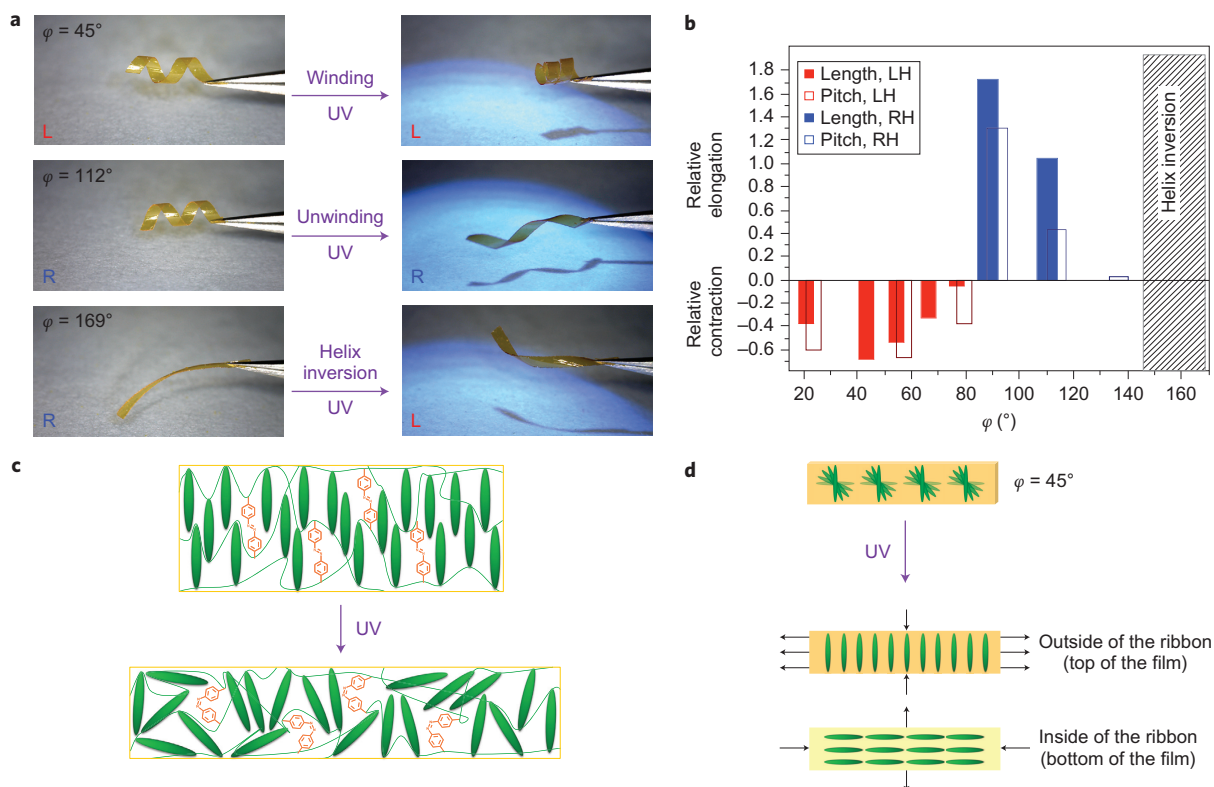
Figure 4 | Photoactuation modes of the polymer springs doped with S-811. a, Spiral ribbons irradiated for two minutes with ultraviolet light ($\lambda = 365$ nm) display isochoric winding, unwinding and helix inversion as dictated by their initial shape and geometry. **b**, A large amplitude contraction is obtained on light-driven winding of ribbons with $\varphi \approx 45°$, and a large amplitude elongation is obtained on light-driven unwinding of ribbons with $\varphi \approx 90°$. LH, left-handed; RH, right-handed. **c**, Under irradiation with ultraviolet light, the ribbons contract along the director and expand in the perpendicular directions, as is consistent with an ultraviolet-induced increase of disorder. **d**, Scheme to represent the mechanisms through which the shape of the ribbons is modified under irradiation with ultraviolet light, for $\varphi = 45°$. The ribbons deform to accommodate the preferred distortion along the main axis of the ribbon, and this preferred distortion is determined by the orientation of the molecules.

and Supplementary Movies 1 and 2). Remarkably, it was also possible to observe inversion of the helical sense from right-handed to left-handed (Fig. 4a). After a few minutes the deformations reached a steady state ($\lambda = 365$ nm at 60 mW cm^{-2}). They were fully reversible at room temperature, with relaxation times of the order of a dozen minutes. With visible light, this reversal process could be accelerated to completion in a few seconds. The winding of the photoresponsive ribbons was associated with remarkably large isochoric contraction (which reached up to about 60% of the original length of the ribbons). For unwinding associated with elongation, amplitudes of up to 40% of the original shape were observed (Fig. 4b). The direction of the actuation (expansion or contraction) and its magnitude are both encoded in the shape and geometry of each spiral ribbon.

Important characteristics of an actuator are rate of response and reversibility. In the case of photoisomerization reactions, the intensity of irradiation constitutes a control parameter for reaction rate. However, it is probable that the rate of the shape reversal is determined by the rate of thermal relaxation of the photoactive dopant, the *cis*-azobenzene molecule. Here, the half-life time for thermal relaxation of the *cis*-azobenzene was about 15 minutes in solution and under ambient light (Supplementary Fig. 1). This half-life corresponds well to the thermal relaxation rate of the ribbons, which suggests that the reorganization of the polymer network is faster than the thermal isomerization of the *cis*-azobenzene. Thus, the relaxation process is probably determined by the specific molecular structure of the photoresponsive switch. The thermal relaxation can be accelerated by irradiation with visible light. We also performed absorption spectroscopy of the films on repeated alternating irradiation with ultraviolet light ($\lambda = 365$ nm) and visible light ($\lambda \geq 420$ nm). Photoswitching of azobenzene **1** is, indeed, reversible, even after being covalently bonded to the polymer network, and there was nearly no fatigue effect on the sample after ten cycles of alternating ultraviolet and visible irradiation (Supplementary Fig. 10).

The mechanical behaviour of the springs depends on the handedness of the director twist and on their angular offset φ (Fig. 3). Earlier studies demonstrated that controlling the geometry of the director and its spatial variation in photoresponsive polymer networks can drive various types of light-induced deformations in these materials[26,30]. Here we show that large deformations are possible by utilizing the twisting mechanism. Understanding this mechanism requires that the specificity of light as a stimulus needs to be taken into account. Both experimental and theoretical investigations have established that irradiating liquid-crystal polymer networks doped with photoresponsive molecules induces disorder and thus leads to anisotropic deformations characterized by contraction in the direction of the director, and expansion in perpendicular directions (Fig. 4c)[37]. As mentioned above, all ribbons curl in such a way that the region that faces the top of the cell during polymerization is always found at the outside of the ribbon, whereas the bottom of the film always ends up inside the twisted ribbon. Having determined the orientation of the molecules on each side of the ribbon before irradiation, an interpretation becomes possible: the ribbons always deform to accommodate the preferred distortion along the main axis of the ribbon, and this preferred distortion is determined by the orientation of the molecules, which is, in turn, determined by the cutting direction.
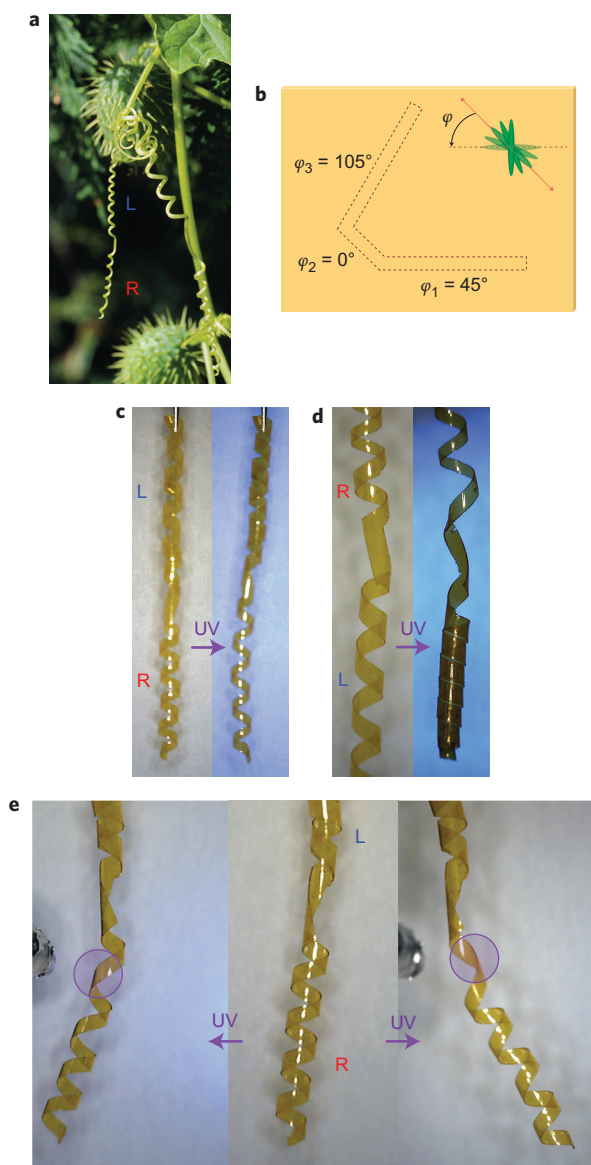
Figure 5 | Mixed-helicity springs doped with S-811 display a complex range of mechanical photoresponses. a, A coiled tendril of the wild cucumber plant. (Image courtesy of Green Thumb Photography/Beth Hoar) **b**, The liquid-crystal polymer film is cut to introduce regions that display different dynamic behaviours. **c,d**, A polymer spring that displays a cucumber tendril-like shape, composed of two oppositely handed helices connected by a kink. On irradiation the right-handed helix unwinds (**c**) and the left-handed helix winds (**d**). **e**, Bending of the spring is achieved and controlled by selective irradiation, which induces a local elongation of the right-handed ribbon. The coloured circles indicate the irradiation spots where elongation occurs.

The mechanism that drives the photoresponse in the ribbons is illustrated for the ribbon where $\varphi = 45°$ (Fig. 4d). Here, the outside face undergoes expansion along its long axis, whereas the inner face shrinks. Both photodeformations accommodate an increase in the twist, as observed experimentally (Fig. 4a). The work provided by such a ribbon can be estimated by attaching a known mass to one of the springs. Under irradiation, the ribbon works against gravity by lifting the mass up (Supplementary Fig. 11). This experiment yielded a value of 3.04 J mol^{-1} of azobenzene (and a power of 9 nW), a similar value to that reported for the work by thin molecular crystals (2.95 J mol^{-1} of a photoresponsive molecule embedded in the crystal)[15]. The similarity between these

values highlights that these soft actuators can perform at least as well as their rigid counterparts. To summarize, the photoresponse of the ribbons at the macroscopic level is determined by the orientation of the molecules within the ribbons. Under irradiation with ultraviolet light, the ribbons contract along the director and expand in the perpendicular directions, as is consistent with an ultraviolet-induced increase of disorder. This mechanism is reminiscent of a design strategy implemented successfully in other photomechanical soft materials: In Aida and co-worker's polymer brushes, irradiation with light unbalances competing strains between the front and back sides of the film, which in turn bends the film[38].

Towards mimicking the mechanical behaviour of plant tendrils. In the movements of plant tendrils, winding and unwinding is understood to be governed by the shrinking and expansion of cell walls orthogonally to each other. In our system, we anticipate that the mechanism of winding and unwinding results from photoisomerization of embedded units of **1** from the *trans*-state to the bent *cis*-state, which contracts the material along and elongates it perpendicular to the director. This proposed mechanism bears considerable resemblance to that believed to occur in biological systems.

In nature, tendrils combine bending and twisting distortion modes to find a support and lift a plant upwards, towards the Sun. A fully operational device cut out of a single sheet of a liquid-crystal polymer network was found to display the type of complex and biologically relevant behaviour that inspired the current approach (Fig. 5). These mixed-helicity springs, which comprise two oppositely handed helices joined at a kink, displayed regions that simultaneously coiled and uncoiled under irradiation (Fig. 5b–d). Noticeably, when a hybrid spring was clamped at both ends and pulled axially, it unwound. Furthermore, localized irradiation of specific sections of these springs led to a bending motion, the direction of which can be also controlled (Fig. 5e).

Finally, the differential behaviour of a mixed-helicity spring was used to demonstrate proof-of-principle for a photomechanical engine that performs a complex mechanical function. To this end, a tendril-like spring was clamped at each end and irradiated alternately with ultraviolet and visible light (Fig. 6). The confinement of the tendril allows the central kink to perform a continuous push–pull motion that is similar to the piston motion essential to the design and functioning of classical mechanical motors. The movement of the spring retained its amplitude over ten cycles (Fig. 6b and Supplementary Movie 3). As a further demonstration of the ability of these materials to produce useful work we attached a simple magnet to the central kink of a tendril-like spring. The material was found to withstand the weight of the magnet ($m \approx 2$ mg) with only a small reduction in mobility, and the movement of this magnet was used to move an additional magnet ($m \approx 0.5$ mg), separated (by ~10 mm) through a glass plate, back and forth in a predictable way that was controlled completely by the mechanical action of the mixed-helicity spring (Fig. 6c and Supplementary Movie 4).

Conclusions
Inspired by biological systems, we designed, synthesized and studied the versatile actuation modes of photoresponsive liquid-crystalline polymer springs. Light operates molecular-scale motion (*cis–trans* photoisomerization), which is converted into large macroscopic deformations of the springs through a mechanism that involves an increase of disorder associated with anisotropic deformations. This molecular approach gives access to (and control of) a large diversity of morphology and photoresponses in the spiral ribbons. More than a single actuation mode is encoded inherently in these chiral objects and the actuation can be reversed when changing from one handedness to the other. Moreover, we have demonstrated
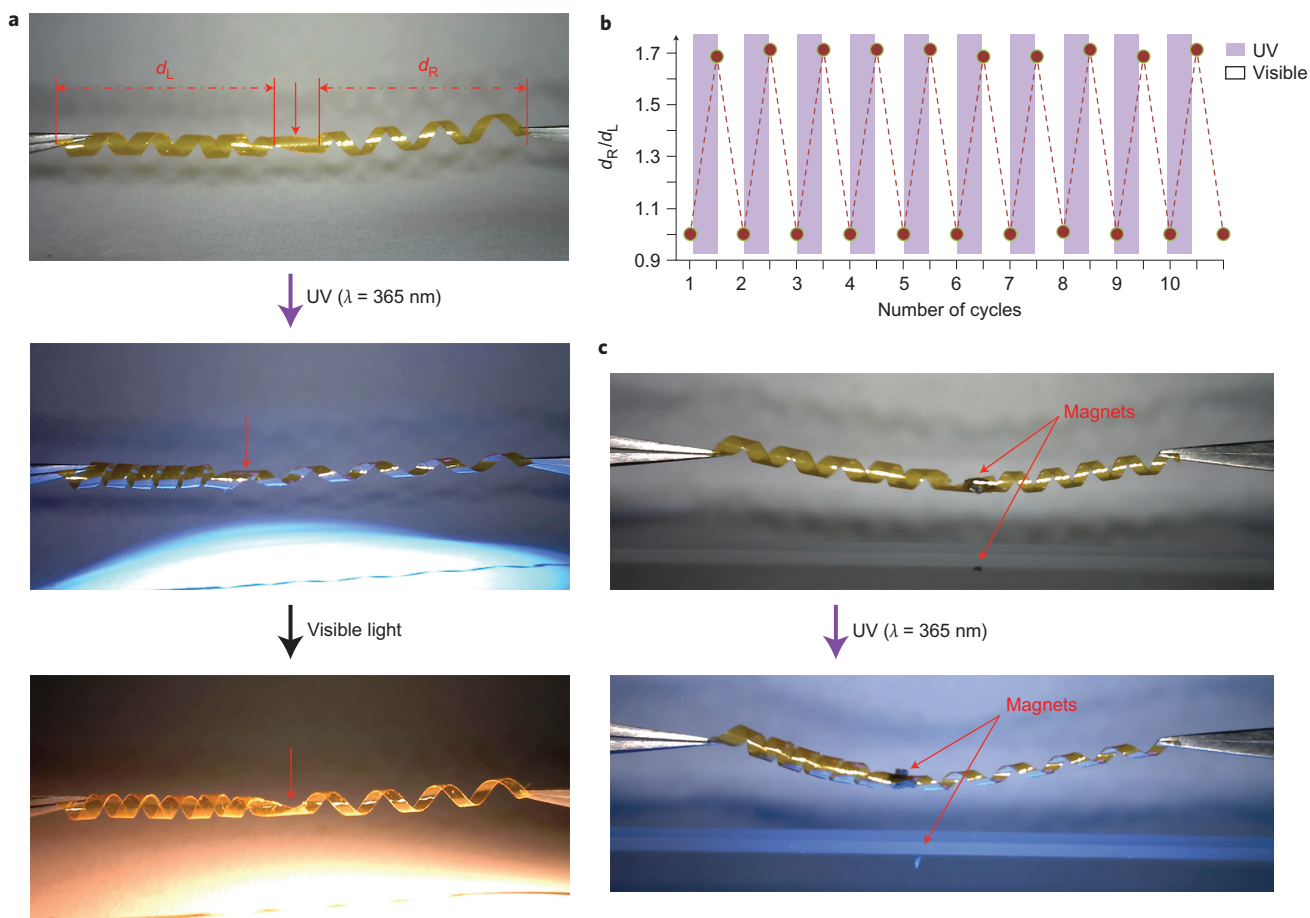
Figure 6 | Proof-of-principle for a mechanical device powered by light. a, On alternate irradiation with ultraviolet and visible light, the central kink of a mixed-helicity ribbon doped with S-811 performs a continuous piston-like motion (Supplementary Movie 3). **b**, The device displays no sign of fatigue over ten cycles of alternating irradiation. **c**, A magnet connected to the kink ($m \approx 2$ mg) undergoes a push–pull shuttling motion, a motion further transmitted to another magnet placed 10 mm below ($m \approx 0.5$ mg).

that these chiral objects can be used to achieve work. These versatile actuators constitute a solid basis for designing novel functional materials that can provide an economic, clean and electrode-less alternative to conventional actuators.

Methods

Materials. Monomers **2**, **3** and **4** were purchased from Synthon Chemicals and mixed in a 3:1:2 ratio by weight. A nematic liquid crystal (E7 Merck), used to prevent crystallization when the mixture was inserted in the cell, was added to the monomer mixture in a ratio of 1:2.5 by weight in favour of the monomer mixture. Molecular switch **1** was synthesized according to reported procedures[39,40], and its photoisomerization in hexane was characterized using a Perkin Elmer Lambda 850. **1** was added in 10 wt% to the matrix described previously. Chiral dopant S-811 or R-811 (Merck) was added to the mixture (0.04 wt%) to induce a cholesteric helix with a pitch of 200 μm. Phenylbis(2,4,6-trimethylbenzoyl)phosphine oxide (Ciba Irgacure 819) was purchased from Sigma-Aldrich and used as a photoinitiator with a 1.0 wt% concentration in the cholesteric mixture. All compounds were dissolved and mixed in dichloromethane purchased from Sigma-Aldrich. Afterwards, the solvent was evaporated at 40 °C under a nitrogen stream. Twist cells with a 50 μm cell gap were either purchased from the Electrical Heating Company or home-made using a Sunever 150 alignment layer from Nissan Chemical Industries. The twist cells were preheated at 55 °C prior to their use and the cholesteric mixture was introduced into the cell at 48 °C. The cell was irradiated from the top using an Edmund MI-150 high-intensity illuminator equipped with a cutoff filter ($\lambda \geq 420$ nm) to initiate the polymerization. After irradiation the cell was left in the oven at 55 °C overnight. An illustration for this procedure is provided in Supplementary Fig. 3. Thermal gravimetric analysis experiments showed that the final ribbon contained ~25% E7 in mass, which suggests all the material that comprised the photoresponsive liquid-crystalline mixture was still present in the final ribbons (Supplementary Fig. 12).

Preparation of the ribbons and structural characterization. The twist cells were frozen with liquid nitrogen and then opened using a scalpel to reveal the polymer film.

The film was cut in different directions to provide ribbons with a variety of shapes. After cutting, the ribbons were dried at 55 °C for two hours. The width of the ribbons was adjusted to ~0.8 mm. The length (L) of the one-handed ribbons was ~0.8–1.3 cm and the length of the mixed-helicity ribbons was ~4 cm. The thicknesses of the ribbons and the molecular organization through the film were evaluated by using scanning electron microscopy. The thicknesses were 43 μm for films prepared in commercial cells and 48 μm for those prepared in home-made cells, in good agreement with the 50 μm gap of the cells that were used. A Hönle blue point light-emitting diode (LED) lamp was used to analyse the photoresponses. Therefore, the polymer ribbon was placed 4 cm below one LED head and irradiated with an intensity that ranged from about 30 mW cm^{-2} to 60 mW cm^{-2}. The light-driven deformations were followed using a Dino-Lite Pro AM4113T USB microscope with ×29 magnification.

References
1. Feynman, R. P. in *Miniaturization* (ed. Gilbert, H. D.) 282–296 (Reinhold, 1961).
2. Drexler, K. E. *Nanosystems: Molecular Machinery, Manufacturing and Computation* (Wiley, 1992).
3. Koumura, N., Zijlstra, R. W. J., van Delden, R. A., Harada, N. & Feringa, B. L. Light-driven monodirectional molecular rotor. *Nature* **401**, 152–155 (1999).
4. Leigh, D. A., Wong, J. K. Y., Dehez, F. & Zerbetto, F. Unidirectional rotation in a mechanically interlocked molecular rotor. *Nature* **424**, 174–179 (2003).
5. Fletcher, S. P., Dumur, F., Pollard, M. M. & Feringa, B. L. A reversible, unidirectional molecular rotary motor driven by chemical energy. *Science* **310**, 80–82 (2005).
6. Balzani, V. *et al.* Autonomous artificial nanomotor powered by sunlight. *Proc. Natl Acad. Sci. USA* **103**, 1178–1183 (2006).
7. von Delius, M., Geertsema, E. M. & Leigh, D. A. A synthetic small molecule that can walk down a track. *Nature Chem.* **2**, 96–101 (2010).
8. Muraoka, T., Kinbara, K. & Aida, T. Mechanical twisting of a guest by a photoresponsive host. *Nature* **440**, 512–515 (2006).

9. Kudernac, T. *et al.* Electrically driven directional motion of a four-wheeled molecule on a metal surface. *Nature* **479**, 208–211 (2011).
10. Lewandowski, B. *et al.* Sequence-specific peptide synthesis by an artificial small-molecule machine. *Science* **339**, 189–193 (2013).
11. Berná, J. *et al.* Macroscopic transport by synthetic molecular machines. *Nature Mater.* **4**, 704–710 (2005).
12. Eelkema, R. *et al.* Nanomotor rotates microscale objects. *Nature* **440**, 163 (2006).
13. Yamada, M. *et al.* Photomobile polymer materials: towards light-driven plastic motors. *Angew. Chem. Int. Ed.* **47**, 4986–4988 (2008).
14. Juluri, B. K. *et al.* A mechanical actuator driven electrochemically by artificial molecular muscles. *ACS Nano* **3**, 291–300 (2009).
15. Morimoto, M. & Irie, M. A diarylethene cocrystal that converts light into mechanical work. *J. Am. Chem. Soc.* **132**, 14172–14178 (2010).
16. Browne, W. R. & Feringa, B. L. Making molecular machines work. *Nature Nanotechnol.* **1**, 25–35 (2006).
17. Ariga, K., Mori, T. & Hill, J. P. Mechanical control of nanomaterials and nanosystems. *Adv. Mater.* **24**, 158–176 (2012).
18. Coskun, A. *et al.* Great expectations: can artificial molecular machines deliver on their promise? *Chem. Soc. Rev.* **41**, 19–30 (2012).
19. Spinks, G. M. Deforming materials with light: photoresponsive materials muscle in on the action. *Angew. Chem. Int. Ed.* **51**, 2285–2287 (2012).
20. Schliwa, M. *Molecular Motors* (Wiley, 2003).
21. Mahadevan, L. & Matsudaira, P. Motility powered by supramolecular springs and ratchets. *Science* **288**, 95–99 (2000).
22. Armon, S., Efrati, E., Kupferman, R. & Sharon, E. Geometry and mechanics in the opening of chiral seed pods. *Science* **333**, 1726–1730 (2011).
23. Gerbode, S. J., Puzey, J. R., McCormick, A. G. & Mahadevan, L. How the cucumber tendril coils and overwinds. *Science* **337**, 1087–1091 (2012).
24. Zhu, L., Al-Kaysi, R. O. & Bardeen, C. J. Reversible photoinduced twisting of molecular crystal microribbons. *J. Am. Chem. Soc.* **133**, 12569–12575 (2011).
25. Kitagawa, D., Nishi, H. & Kobatake, S. Photoinduced twisting of a photochromic diarylethene crystal. A*ngew. Chem. Int. Ed.* **52**, 9320–9322 (2013).
26. Lee, K. M. *et al.* Photodriven, flexural–torsional oscillation of glassy azobenzene liquid crystal polymer networks. *Adv. Funct. Mater.* **21**, 2913–2918 (2011).
27. Warner, M. & Terentjev, E. M. *Liquid Crystal Elastomers* (Oxford Univ. Press, 2003).
28. Natansohn, A. & Rochon, P. Photoinduced motions in azo-containing polymers. *Chem. Rev.* **102**, 4139–4175 (2002).
29. Yu, Y., Nakano, M. & Ikeda, T. Directed bending of a polymer film by light. *Nature* **425**, 145 (2003).
30. Van Oosten, C. L., Bastiaansen, C. W. M. & Broer, D. J. Printed artificial cilia from liquid-crystal network actuators modularly driven by light. *Nature Mater.* **8**, 677–682 (2009).
31. Van Oosten, C. L., Harris, K. D., Bastiaansen, C. W. M. & Broer, D. J. Glassy photomechanical liquid-crystal network actuators for microscale devices. *Eur. Phys. J. E* **23**, 329–336 (2007).
32. Sawa, Y. *et al.* Shape selection of twist-nematic-elastomer ribbons. *Proc. Natl Acad. Sci. USA* **108**, 6364–6368 (2011).
33. Sawa, Y. *et al.* Shape and chirality transitions in off-axis twist nematic elastomer ribbons, *Phys. Rev. E* **88**, 022502 (2013).
34. Teresi, L. & Varano, V. Modeling helicoid to spiral-ribbon transitions of twist-nematic elastomers. *Soft Mater* **9**, 3081–3088 (2013).
35. Forterre, Y. & Dumais, J. Generating helices in nature. *Science* **333**, 1715–1716 (2011).
36. van Oosten, C. L. *et al.* Bending dynamics and directionality reversal in liquid crystal network photoactuators. *Macromolecules* **41**, 8592–8596 (2008).
37. Harris, K. D. *et al.* Large amplitude light-induced motion in high elastic modulus polymer actuators. *J. Mater. Chem.* **15**, 5043–5048 (2005).
38. Hosono, N. *et al.* Large-area three-dimensional molecular ordering of a polymer brush by one-step processing. *Science* **330**, 808–811 (2010).
39. Mossety-Leszczak, B., Wlodarska, M., Galina, H. & Bak, G. W. Comparing liquid crystalline properties of two epoxy compounds based on the same azoxy group. *Mol. Cryst. Liq. Cryst.* **490**, 52–66 (2008).
40. Li, C. *et al.* Synthesis of a photoresponsive liquid-crystalline polymer containing azobenzene. *Macromol. Rapid Commun.* **30**, 1928–1935 (2009).

Acknowledgements

Author contributions

N.K. and S.P.F. conceived the research. N.K., T.K. and J.L.M.C. guided the research. S.I. and B.M. synthesized **1**. S.I., S.J.A. and B.M. carried out the experiments. All authors discussed the results and commented on the manuscript at all stages.

Additional information

Supplementary information and chemical compound information are available in the online version of the paper. Reprints and permissions information is available online at www.nature.com/reprints. Correspondence and requests for materials should be addressed to S.P.F. and N.K.

Competing financial interests

The authors declare no competing financial interests.